https://doi.org/10.2352/ISSN.2470-1173.2020.10.IPAS-180

Color Restoration of Multispectral Images: Near-Infrared (NIR) filter-to-Color (RGB) image

THAWEESAK TRONGTIRAKUL, Dept. Electronics and Telecommunication Engineering, Faculty of Engineering, King Mongkut's University of Technology Thonburi, Bangkok, Thailand
WERAPON CHIRACHARIT, Dept. Electronics and Telecommunication Engineering, Faculty of Engineering, King Mongkut's University of Technology Thonburi, Bangkok, Thailand
SOS AGAIAN, Dept. Computer Sciences, CUNY Graduate Center & College of Staten Island, New York, USA

Abstract

Multispectral images captured by near-infrared (NIR) filtered devices have an attractive potential for numerous applications in computer vision, robot vision, and an artificial intelligence system. Although near-infrared (NIR) filtered devices display some unseen details, but their colors contain false colors affected main color components. Therefore, the color restoration of near-infrared (NIR) filtered images is a challenge for human perception. To overcome the challenge, the proposed method has four main steps: i) color balance with chromatic adaptation; ii) color component switching; iii*) Hue-Saturation-Lightness adjustment; and iv) image fusion using a proportional-weighing metric. The proposed results achieve to: i) restore RGB color component, ii) remove the color-overlapped effect and generate structure details close to the ground truth images; and iii) preserve overall brightness.*

Introduction

The computer vision and its related field are dramatically expanding in different directions. Among technological advancements in hardware and artificial intelligence (AI) capabilities, they have generated much new distance in an extensive range of applications. Currently, there are several devices that are capable of capturing the visual details [1] in different spectral bands, which cover visible wavelengths and infrared band [2]. Traditional image processing algorithms (image enhancement, segmentation, haze removal, super-resolution, color restoration, image re-coloring, image and video compression [3-6]) use advantages of multispectral technology. Currently, RGBN images can be used in many applications related to image compression [7], color restoration [8], and image denoising [9].

Fig. 1 illustrates the issues of infrared-filter images. The scene illustrates several colors in the outdoor that is reflected by intense sunlight (near the infrared radiation). The details in dark green (see Fig. 1(a)) can be observed by an infrared-filter image (see Fig. 1(b)). The intensity distribution of an infrared-filter image has the relationship to red and green components when luminance is less than 190, and to green and blue components, when luminance level is more than 190 (see Fig. 1(c)). In addition, it can be noticeable that visible wavelength components (RGB-components) are expanded through 700 *nm* to 1000 *nm*, approximately [10] (see Fig. 1(d)).

The construction of a chromatic image with color-component images depends on several factors, for instance, ambient light, surface reflection, and sensors [1, 11]. All factors related to a wavelength (λ), which turn a multispectral image having components as $\{C_\lambda\} = \{R_\lambda \cup G_\lambda \cup B_\lambda \cup IR_\lambda\}$. $C_{(\cdot)}$ denotes a chromatic image, composed of red - $R_{(\cdot)}$, green - $G_{(\cdot)}$ and blue - $B_{(\cdot)}$ components with additional infrared-filter component - $IR_{(\cdot)}$.

a) ground truth image

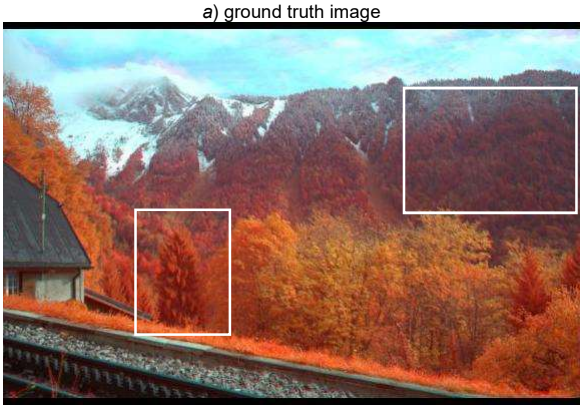

b) infrared-filter image

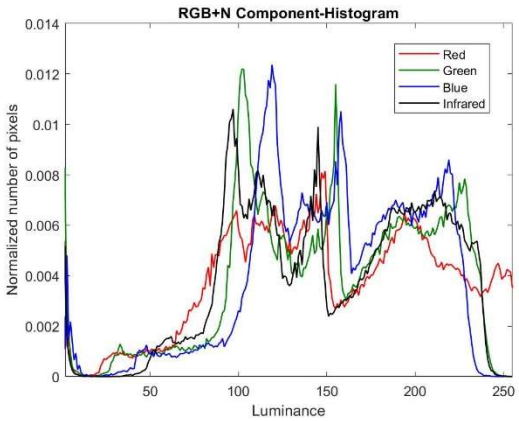

c) RGB+N histogram

Figure 1. The effect of color component changed by an infrared-filter.

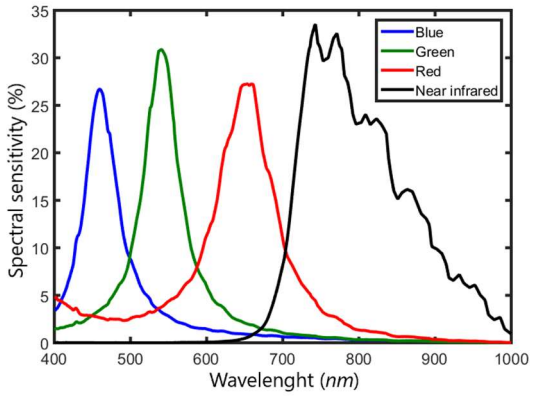

d) Spectral sensitivity comparison with RGB and NIR [10]

Figure 1(Continued). The effect of color component changed by an infrared-filter.

The multispectral image with an infrared-filter component is commonly used in many applications, such as surveillance, night-vision images, and thermal images. The objective of the RGB color restoration is to acquire an image in the visible spectral range (400 – 700 *nm*).

Most applications mentioned above are based on the use of binocular, one for the visible wavelength and another one for near-infrared band. In fact, visible wavelength sensors generate color scenes with noise and motion blur while infrared sensor generates the monochrome image with extensive details and fewer noises. Therefore, *a*) color restoration and *b*) noise deduction can be challenging tasks.

This paper present the color restoration of multispectral images: near-infrared (NIR) filter-to-color (RGB) image based on the novel color-component switching. It is less complexity, making proper for real-time applications like surveillances or video interactive devices. The rest of the paper is organized as follows: Section 2 presents the proposed method to restore color-components. Section 3 introduces computer simulation and experimental results. Finally, Section 4 offers the conclusion and ideas that can be applied for commercial applications.

1. Take an input infrared-filter image
2. Apply a color balance to the input image
3. Switch color components of the color-balanced image
4. Apply a color balance to the switched color-component image
5. Adjust Hue-Saturation-Lightness (HSL) of the color-balanced image in step 4
6. Calculate the proportional-weighing metric by using the input image
7. Generate an RGB image by fusing the HSL-adjusted image and the input infrared-filter image with adaptive weighing metric
8. Obtain an output RGB image

Figure. 2. The proposed framework

Proposed Method

In this section, we introduce the framework to restore RGB color for infrared-filter images. It has four main steps (see Fig. 2): *i*) color balance; *ii*) color component switching; *iii*) Hue-Saturation-Lightness adjustment; and *iv*) image fusion using a proportional-weighing metric.

Color balance with chromatic adaptation

Let $I_{i,j,k}$ be infrared-filter photography and μ_k is the average luminance of the k^{th} color component. The concept of the color balance with chromatic adaption [13] can be defined as:

$$\begin{bmatrix} CB_{i,j,1} \\ CB_{i,j,2} \\ CB_{i,j,3} \end{bmatrix} = \begin{bmatrix} \mu_1 \\ \mu_2 \\ \mu_3 \end{bmatrix} \begin{bmatrix} I_{i,j,1} \\ I_{i,j,2} \\ I_{i,j,3} \end{bmatrix} \quad (1)$$

where k = 1, 2 and 3 represent a red, a green and a blue component, respectively.

Color component switching

In general, infrared-filter photography has false colors. For example, the red component is preserved by an infrared filter, the green color becomes red, and the white component is transformed by a blue component (see Fig. 2). Therefore, the swapping of color components is very important at this stage. It can be calculated as:

$$S_{i,j,k} = \begin{cases} \underset{k}{\text{mean}}\{\rho_r CB_{i,j,k}, \rho_g CB_{i,j,k}, \rho_b CB_{i,j,k}\}, & k = 1 \\ \underset{k}{\text{mean}}\{\gamma_r CB_{i,j,k}, \gamma_g CB_{i,j,k}, \gamma_b CB_{i,j,k}\}, & k = 2 \\ \underset{k}{\text{mean}}\{\beta_r CB_{i,j,k}, \beta_g CB_{i,j,k}, \beta_b CB_{i,j,k}\}, & k = 3 \end{cases} \quad (2)$$

where $\rho_{(\cdot)}, \gamma_{(\cdot)}$ and $\beta_{(\cdot)}$ are color constant, $0 \le \rho_{(\cdot)}, \gamma_{(\cdot)}, \beta_{(\cdot)} \le 1$. $(\cdot)_r, (\cdot)_g$ and $(\cdot)_b$ represent a red, a green and a blue component, respectively.

Hue-Saturation-Lightness (HSL) adjustment

For some color correction method, for instance, scaling on a very narrow color-distributed range. The proposed HSL can be adjusted in a board color-distributed range and can be calculated as:

$$HSL_{i,j,k} = \begin{cases} \frac{H_{i,j} - \min\{H_{i,j}\}}{\max\{H_{i,j} - \min\{H_{i,j}\}\}}, & k = 1 \\ \frac{S_{i,j} - \min\{\ _{i,j}\}}{\max\{S_{i,j} - \min\{S_{i,j}\}\}}, & k = 2 \\ \frac{L_{i,j} - \min\{L_{i,j}\}}{\max\{L_{i,j} - \min\{L_{i,j}\}\}}, & k = 3 \end{cases} \quad (3)$$

where $H_{i,j}, S_{i,j}$ and $L_{i,j}$ are a hue, a saturation, and a lightness component, respectively.

Image fusion using a proportional-weighing metric

In this sub-section, we attempt to restore the blue component form an input infrared-filter image. The proportion of the blue component can be calculated as:

$$\omega_{i,j} = \frac{I_{i,j,k}}{L-1} \quad ; \quad k = 3 \quad (4)$$

where $I_{i,j,k}$ is an input infrared-filter image. L is the total luminance levels of a blue component.

The proportional-weighing metric can be applied by fusing the two images: color image adjusted by an HSL color-component image and the input infrared-filter image. The calculation of an image fusion can be described as:

$$F_{i,j,k} = \begin{cases} RGB_{i,j,k}^{Adj}, & k = 1 \\ RGB_{i,j,k}^{Adj}, & k = 2 \\ \omega_{i,j} \cdot RGB_{i,j,k}^{Adj} + (1 - \omega_{i,j}) I_{i,j,k}, & k = 3 \end{cases} \quad (5)$$

where $RGB_{i,j,k}^{Adj}$ is the color image adjusted by an HSL color-component image. $\omega_{i,j}$ is a proportional-weighing metric

Experimental Results

This section explains the evaluation procedure and the performance of the proposed framework. For infrared-filter images and testing process, as mentioned below, the test images are available at: RGB-NIR Scene Dataset, Image and Visual Representation Lab (IVRL) [14]. The image size is: 382×576 in RGB file format (ground truth) and IR file format (infrared-filter images).

Because of the fact that there are any no standard methods to evaluate the performance of an infrared-filter removal, we use three measures: *i*) colorfulness (CF) [15-16], *ii*) structural similarity index metric (SSIM) [17], and *iii*) logarithmic luminance error (LLE) [18-19], which are widely used in color-related literature. These results can be observed subjectively in Table I-III and objectively in Fig. 3.

Colorfulness (CF)

It is one qualification of the chrominance feature that humans comprehend. [20-21] introduced a linear colorfulness function, but human perceptions are not linear. Therefore, it is reasonable to use a non-linear function for estimating colorfulness, corresponding to the human visual system (HVS) [15-16].

$$CF = 50log^{\gamma}\left(\frac{\sigma_{\alpha}^2}{|\mu_{\alpha}|^{0.2}}\right) log^{\gamma}\left(\frac{\sigma_{\beta}^2}{|\mu_{\beta}|^{0.2}}\right) \quad (6)$$

$$\mu_{(\cdot)} = \frac{1}{2N}\left(\sum_{i=1}^{N}\alpha_i + \sum_{i=1}^{N}\beta_i\right) \quad (7)$$

$$\sigma_{(\cdot)}^2 = \frac{1}{2N}\left(\sum_{i=1}^{N}\left(\alpha_{(\cdot)}^2 - \mu_{(\cdot)}^2\right) + \sum_{i=1}^{N}\left(\beta_{(\cdot)}^2 - \mu_{(\cdot)}^2\right)\right) \quad (8)$$

$$\alpha = R - G \;\; ; \;\; \beta = 0.5(R+G) - B \quad (9)$$

where R, G and B are red, green, and blue components. N represents the total number of pixels. γ is a power factor.

Structural similarity index metric (SSIM)

It is a measure for estimating the perceived quality in digital images. SSIM is the measure of perception that considers image deterioration related to structural data changes including luminance and contrast attributes.

$$SSIM = \frac{(2\mu_G\mu_R + c_1)(2\sigma_{GR} + c_2)}{(\mu_G^2\mu_R^2 + c_1)(\sigma_G^2\sigma_R^2 + c_2)} \quad (10)$$

$$c_1 = (0.01L)^2 \;\; ; \;\; c_2 = (0.03L)^2 \quad (11)$$

where L denotes the total luminance levels. σ_{IR} represents the covariance of an input infrared-filter image and a resulting color image. μ is the averaging luminance and $\sigma^2$is variance. $(\cdot)_G$ and $(\cdot)_R$ represent a ground truth image and a resulting color image, respectively.

Logarithmic luminance error (LLE)

Logarithmic luminance error (LLE) is the cross-averaging luminance measure between two images. The measure estimates the performance in preserving the reference image brightness. Also, we calculate the measure in a logarithmic term due to the perception of the human visual system (HSV).

$$LLE = log^{\gamma}|\mu_G - \mu_R| \quad (12)$$

where μ_G and μ_R are the averaging luminance of a ground truth image and a resulting color image, respectively. γ denotes a power factor.

Table I-III show the performance of colorfulness (CF), structural similarity index metric (SSIM), and logarithmic luminance error (LLE). The infrared-filter images get the worst results. Just two images have the similarity index close to the ground truth images more than 75.4% as shown in Table II. The proposed color restoring images obtain the best image quality assessment. The colorfulness in Table I shows the high number corresponding to Fig. 3. Similarity index estimates the structural similarity up to 82.87%. The proposed-resulting images in Fig. 3 show non-color overlapped edges while some infrared-filter images have color-overlapped edges. Luminance error in Table III shows the brightness preservation performance. The proposed method preserves overall brightness close to the ground truth images.

Table I Colorfulness (CF) [15-16]

Name	Infrared-filter images	Ground truth images	Proposed images
Forest	8.2096	10.7602	10.2164
River	6.9599	11.2101	42.7649
Street	4.9067	10.1386	14.6335
Urban	5.8480	17.3311	15.6551
Lake	5.2064	8.0668	16.4969
Moutain	5.7444	8.3932	15.1921

Table II Structural similarity index metric (SSIM) [17]

Name	Infrared-filter images	Proposed images
Forest	0.5534	0.6987
River	0.7540	0.7542
Street	0.4136	0.8235
Urban	0.5093	0.7564
Lake	0.6185	0.8287
Moutain	0.7713	0.8032

Table III Logarithmic luminance error (LLE) [18-19]

Name	Infrared-filter images	Proposed images
Forest	2.0364	0.8287
River	2.5286	1.0281
Street	1.7460	1.0183
Urban	2.0699	1.0657
Lake	2.0559	1.1202
Moutain	2.7051	0.9865

Color restoration of multispectral images: near-infrared (NIR) filtered-to-color (RGB) image is a challenging image processing with many color effects. The amount of infrared-filter component impacting RGB components depends on many factors, for instance, ambient light, surface reflection, and some kinds of sensors. The proposed method achieves to: *i*) restore RGB color component, *ii*) remove the color-overlapped effect and generate structure details close to the ground truth images; and *iii*) preserve overall brightness.

The proposed method can be applied for many near inferred-based applications such as surveillances, food-processing applications, military applications, computer graphic programs, video-interactive applications, entertainment applications, etc

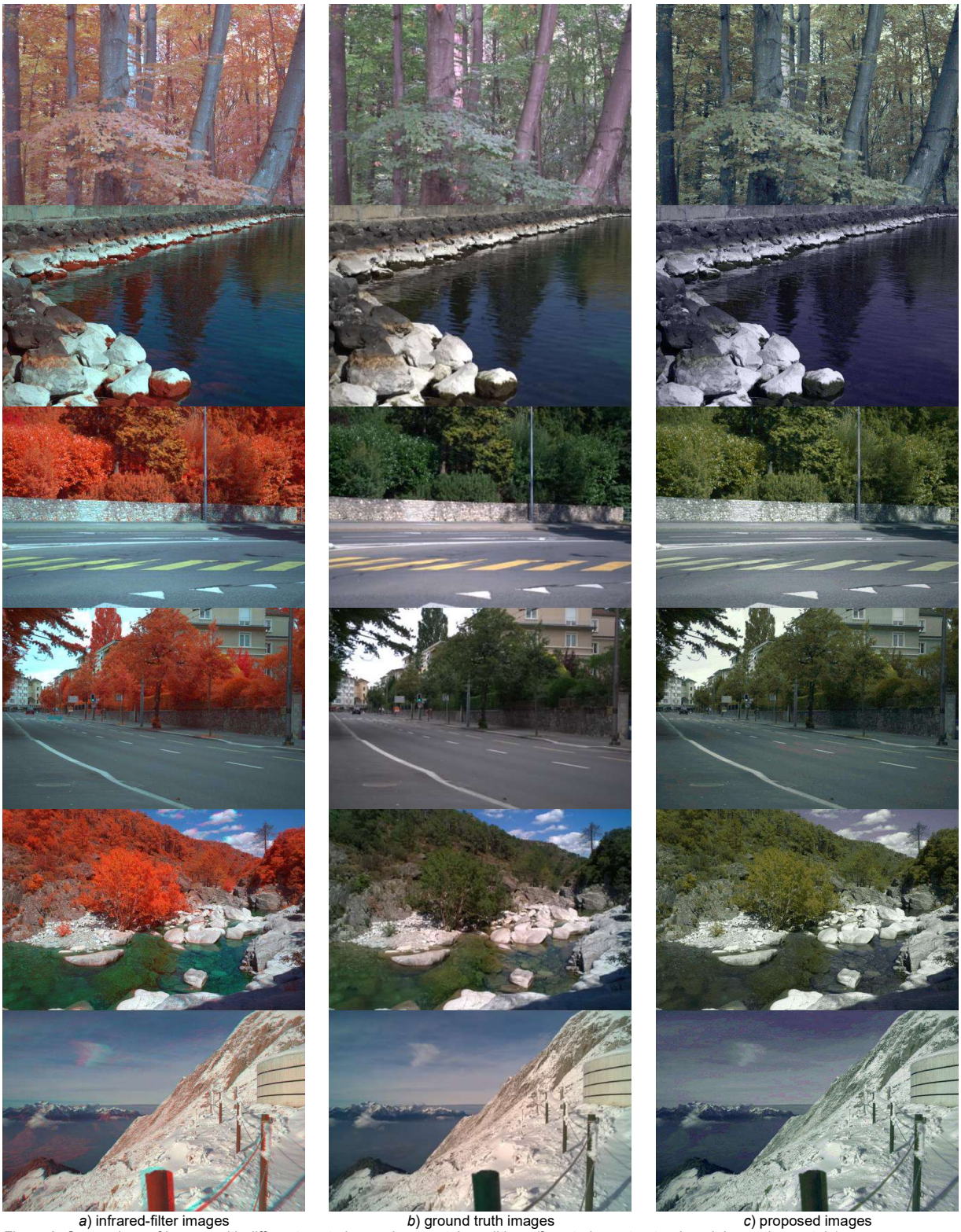

a) infrared-filter images *b*) ground truth images *c*) proposed images

Figure 3. Comparison of images with different capturing environmental conditions (forest, river, street, urban, lake, and mountain) forest_0058, water_0001, street_0042, street_0038, water_0027, mountain_0040

Acknowledgment

Special thanks to National Science and Technology Development Agency (NSTDA) for the education sponsorship grant. This work was partially supported by facilities grants to access the facilities in the industrial education, Rajamangala University of Technology Phra Nakhon (RMUTP).

References

[1] X. Soria, A. D. Sappa and A. Akbarinia, "Multispectral single-sensor RGB-NIR imaging: New challenges and opportunities," 2017 Seventh International Conference on Image Processing Theory, Tools and Applications (IPTA), Montreal, QC, 2017, pp. 1-6.

[2] U. Kayıkcı, E. Oduncu, M. Sivaslıgil and B. Aytaç, "Flare signature analysis in infrared band," 2017 25th Signal Processing and Communications Applications Conference (SIU), Antalya, 2017, pp. 1-4.

[3] M. Roopaei, S. Agaian, M. Shadaram and F. Hurtado, "Cross-entropy Histogram Equalization," 2014 IEEE International Conference on Systems, Man, and Cybernetics (SMC), San Diego, CA, 2014, pp. 158-163.

[4] L. Huang, J. Yin, B. Chen and S. Ye, "Towards Unsupervised Single Image Dehazing With Deep Learning," 2019 IEEE International Conference on Image Processing (ICIP), Taipei, Taiwan, 2019, pp. 2741-2745.

[5] A. Montaldo, L. Fronda, I. Hedhli, G. Moser, S. B. Serpico and J. Zerubia, "Causal Markov Mesh Hierarchical Modeling for the Contextual Classification of Multiresolution Satellite Images," 2019 IEEE International Conference on Image Processing (ICIP), Taipei, Taiwan, 2019, pp. 2716-2720.

[6] Ponomarenko, Mykola, Miroshnichenko, Oleksandr; Lukin, Vladimir, Egiazarian, Karen, "Electronic Imaging," Image Processing: Algorithms and Systems XVII, pp. 263-1-263-7(7).

[7] N. Salamati, Z. Sadeghipoor and S. Süsstrunk, "Compression of multispectral images: Color (RGB) plus near-infrared (NIR)," 2012 IEEE 14th International Workshop on Multimedia Signal Processing (MMSP), Banff, AB, 2012, pp. 65-70.

[8] Chulhee Park and Moon Gi Kang, "Color Restoration of RGBN Multispectral Filter Array Sensor Images Based on Spectral Decomposition," 2016 Imaging: Sensors and Technologies, vol.16, no. 5, 719.

[9] H. Yamashita, D. Sugimura and T. Hamamoto, "RGB-NIR imaging with exposure bracketing for joint denoising and deblurring of low-light color images," 2017 IEEE International Conference on Acoustics, Speech and Signal Processing (ICASSP), New Orleans, LA, 2017, pp. 6055-6059.

[10] Spectral Devices Inc: https://www.spectraldevices.com/products/multispectral-camera-rgb-and-nir-bands: accessed on August 29, 2019.

[11] X. Yang, H. Li, Y. Fan and R. Chen, "Single Image Haze Removal via Region Detection Network," in IEEE Transactions on Multimedia.

[12] Dümbgen, Frederike; Helou, Majed El; Gucevska, Natalija; Süsstrunk, Sabine, "Near-Infrared Fusion for Photorealistic Image Dehazing," Color Imaging XXIII: Displaying, Processing, Hardcopy, and Applications, pp. 321-1-321-5(5).

[13] Bruce Lindbloom, www.brucelindbloom.com/index.html?EqnChromAdapt.html: accessed on August 29, 2019

[14] RGB-NIR Scene Dataset, Image and Visual Representation Lab (IVRL), https://ivrl.epfl.ch/research-2/research-downloads/supplementary_material-cvpr11-index-html: accessed on August 29, 2019.

[15] C. Gao, K. Panetta and S. Agaian, "No reference color image quality measures," 2013 IEEE International Conference on Cybernetics (CYBCO), Lausanne, 2013, pp. 243-248.

[16] K. Panetta, C. Gao and S. Agaian, "No reference color image contrast and quality measures," in IEEE Transactions on Consumer Electronics, vol. 59, no. 3, pp. 643-651, August 2013.

[17] Zhou, W., A. C. Bovik, H. R. Sheikh, and E. P. Simoncelli. "Image Qualifty Assessment: From Error Visibility to Structural Similarity." IEEE Transactions on Image Processing. Vol. 13, Issue 4, April 2004, pp. 600–612.

[18] S. Kansal, S. Purwar and R. K. Tripathi, "Trade-off between mean brightness and contrast in histogram equalization technique for image enhancement," 2017 IEEE International Conference on Signal and Image Processing Applications (ICSIPA), Kuching, 2017, pp. 195-198.

[19] N. A. I. S. M. Shukri, K. S. Sim and J. W. Leong, "Minimum mean brightness error quad histogram equalization for scanning electron microscope images," 2016 International Conference on Robotics, Automation and Sciences (ICORAS), Ayer Keroh, 2016, pp. 1-6.

[20] Y.-Y. Fu, "Color image quality measures and retrieval," Ph.D. thesis, Department of Computer science, New Jersey Institute of Technology, January 2006.

[21] D. Haster and S. E. Suesstrunk, "Measuring colorfulness in natural images," Electronic Imaging 2003, 2003, pp. 87-95.

Author Biography

Thaweesak Trongtirakul received the M.Eng. degree in instrumentation engineering from King Mongkut's Institute of Technology Ladkrabang, Bangkok, Thailand. He is studying in D.Eng. Degree in Electronics and Telecommunication at the King Mongkut's University of Technology Thonburi, Thailand. His primary research interests are in computer vision, machine vision, optical images, and smart cities.

Werapon Chiracharit received B.Eng. in Electronic and Telecommunication Engineering in 1999, M.Eng. in Electrical Engineering in 2001, and Ph.D. in Electrical and Computer Engineering in 2007 from King Mongkut's University of Technology Thonburi (KMUTT), Thailand. Currently, he is an assistant professor in the Department of Electronic and Telecommunication Engineering, KMUTT. His research interests include digital image processing and computer vision.

SOS S. AGAIAN is currently a Distinguished Professor with The City University of New York/CSI. He is also listed as a co-inventor on 44 patents/disclosures. The technologies that he invented have been adopted by multiple institutions, including the U.S. Government, and commercialized by industry. He has authored more than 650 technical articles and 10 books in these areas. He is a Fellow of the SPIE, IS&T, and AAAS. He also serves as a Foreign Member for the Armenian National Academy. He received MAEStro Educator of the Year from the Society of Mexican American Engineers. He received the Distinguished Research Award from The University of Texas at San Antonio. He was a recipient of the Innovator of the Year Award, in 2014, of the Tech Flash Titans-Top ResearcherAward San Antonio Business Journal, in 2014, the Entrepreneurship Award (UTSA-2013 and 2016), and the Excellence in Teaching Award, in 2015. He is an Editorial Board Member of the Journal of Pattern Recognition and Image Analysis and an Associate Editor for several journals, including the IEEE TRANSACTIONS ON IMAGE PROCESSING, the IEEE TRANSACTIONS ON SYSTEMS, MAN, AND CYBERNETICS, the Journal of Electrical and Computer Engineering (Hindawi Publishing Corporation), the International Journal of Digital Multimedia Broadcasting (Hindawi Publishing Corporation), and the Journal of Electronic Imaging (SPIE, IS&T).

JOIN US AT THE NEXT EI!

IS&T International Symposium on

Electronic Imaging

SCIENCE AND TECHNOLOGY

Imaging across applications . . . Where industry and academia meet!

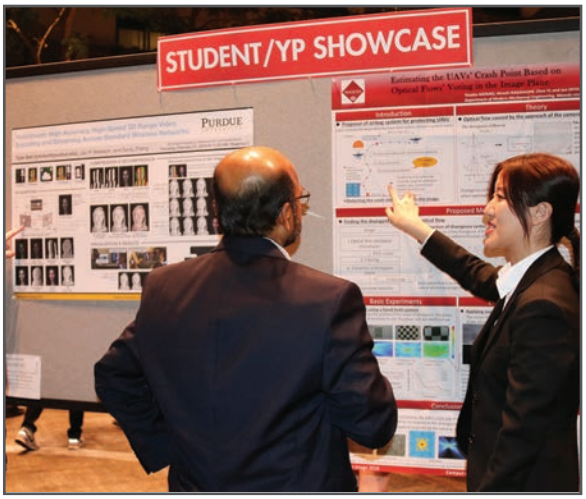

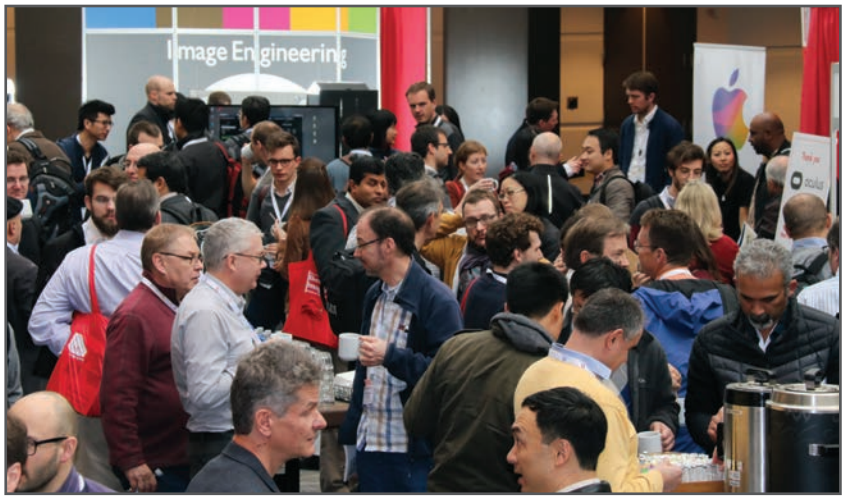

• SHORT COURSES • EXHIBITS • DEMONSTRATION SESSION • PLENARY TALKS •
• INTERACTIVE PAPER SESSION • SPECIAL EVENTS • TECHNICAL SESSIONS •

www.electronicimaging.org

IS&T
imaging.org